Ionics (2015) 21:3141–3149
DOI 10.1007/s11581-015-1558-0

SHORT COMMUNICATION

Control of calcium oxalate morphology through electrocrystallization as an electrochemical approach for preventing pathological disease

Andrónico Neira-Carrillo[1,2] · Patricio Vásquez-Quitral[1] · Marianela Sánchez[1] · Andrés Vargas-Fernández[1] · Juan Francisco Silva[3]

Received: 13 June 2015 / Revised: 14 September 2015 / Accepted: 17 September 2015 / Published online: 28 September 2015

Abstract Pathological crystallization of calcium oxalate (CaOx) inside the urinary tract is called calculi or kidney stone (Urolithiasis). CaOx exhibits three crystalline types in nature: CaOx monohydrate COM, dihydrate COD and trihydrate COT. COD and COM are often found in urinary calculi, particularly COM. Electrocrystallization has been recently used to perform oriented crystallization of inorganic compounds such as Ca-salts. Although many mineralization methods exist, the mechanisms involved in the control of CaOx polymorphism still remain unclear. Herein, we induced selective electrocrystallization of COD by modifying the electrical current, time and electrochemical cell type. By combining above factors, we established an efficient method without the use of additives for stabilizing non-pathological CaOx crystals. We found notorious stabilization of CaOx polymorphisms with hierarchically complex shape with nano-organization assembly, size and aggregated crystalline particles. Our results demonstrated that, by using an optimized electrochemical approach, this technique could have great potential for studying the nucleation and crystal growth of CaOx through functionalized synthetic polymers, and to develop a novel pathway to evaluate new calculi preventing-compound inhibitors.

✉ Andrónico Neira-Carrillo
aneira@uchile.cl

[1] Faculty of Veterinary and Animal Sciences, University of Chile, Av. Santa Rosa, 11735 Santiago, Chile

[2] Advanced Center for Chronic Diseases (ACCDiS), University of Chile, Santiago, Chile

[3] Departamento de Química de los Materiales, Laboratorio de Electrocatálisis, Facultad de Química y Biología, Universidad de Santiago de Chile, Santiago, Chile

Keywords Mineralization · Electrocrystallization · Urolithiasis · Calcium oxalate · Polymorphism

Introduction

Biological mineralization (Biomineralization) is a very old process by which living organisms produce hierarchical inorganic-organic hybrid materials. Thus, biomineralization refers to the formation of biominerals of biological origin, such as vertebrate bone and teeth, invertebrate shells and exoskeletons, and even mineral particles secreted by plants and bacteria [1]. Biomineralized materials have various functions such as defense, detoxification and protection, among others. These advanced materials often provide greater rigidity and strength to some biomineralized tissues, which have major inorganic and minor organic components. In the urinary calculi and biomineralization context, the urinary stones may be regarded as an example of biomineralization that involves the formation of inorganic minerals by living organisms [2]. However, kidney stone (KS) is a pathological manifestation of this phenomenon, exhibiting features typical of uncontrolled biomineralization of calcium oxalate (CaOx) [3]. Therefore, biominerals can also arise from pathological conditions, such as: atherosclerotic plaque, gallstones, and kidney stones formation or nephrolithiasis. Pathological manifestation inside the urinary tract occurs in pets and humans, and in both the involved inorganic mineral is the CaOx [4]. CaOx is one of the most abundant biominerals in superior plants and represents the most abundant inorganic compound found in mammal urinary calculi, including humans [5]. The prevalence of nephrolithiasis is approximately 6 % in women and 12 % in men in USA [6].

On the other hand, CaOx can crystallize into three forms or polymorphs in nature: as monoclinic CaOx monohydrate

COM ($CaC_2O_4 \cdot H_2O$), tetragonal dihydrate COD ($CaC_2O_4 \cdot 2H_2O$) and triclinic trihydrate COT ($CaC_2O_4 \cdot 3H_2O$) [7, 8]. Nevertheless, only the monohydrate form is thermodynamically stable. Thus, in kidney stones, the first two forms are most commonly found in urinary calculi, where COD has the shape of square base bipyramid, while COM and COT are prism slightly tilted parallelepiped. Low temperatures are required to obtain the trihydrate form. In turn, the polymorphs differ in size. COM has approximated average size of 5.0× 2.0 μm and COD of 1.2×2.7 μm. COD is found in a nether proportion than COM. COM has a high ability to form aggregates that are added to renal tubular cells, favoring the formation of KS. On the contrary, the stabilization of COD crystals by adsorption of urinary molecules avoids the formation KS decreasing the urolithiasis risk by CaOx [9].

Urolithiasis inhibitors are agents that delay various aspects involved in the formation of KS such as nucleation, crystal growth, aggregation and adhesion to renal epithelial cells, etc. [10]. A number of studies have been carried out to investigate the effects of additives on nucleation, crystal growth, aggregation and phase transformation of CaOx hydrates. In this context, CaOx controlled-crystallization has been mainly studied in organic systems, including: Langmuir monolayers [11, 12], vesicles [13], surfactants micelles [14], citrate, amino acids, anionic polyelectrolytes, synthetic molecules [15], and natural macromolecules. Other studies have addressed the presence of natural inhibitors in urine, describing the involvement of both low molecular weight (Mw) molecules such as pyrophosphate, citrate, magnesium, among others and high Mw macromolecules such as glycosaminoglycan (chondroitin sulfate or heparan sulfate), Osteopontin protein (OPN), Tamm-Horsfall protein (THP), nefrocalcina (NC), urinary fragment 1 prothrombin (UPTF-1), etc.

While electrodeposition can be used to direct oriented crystallization of organic or inorganic compounds [16–19], there are studies concerning the polymorphism control by using electrocrystallization. We believe that electrocrystallization represents a very good model to investigate the transformation of cluster to amorphous precursor materials, time deposition, metastable crystalline polymorphs and to study the effect of crystallization conditions on polymorphism selection with tremendous implications for understanding of biomineralization and of crystallization. With this in mind, electrocrystallization technique should become as a novel deposition method for controlling the micro or nanocrystallized inorganic deposition and amorphous precursors in the classical and non-classical crystallization [4, 20, 21]. It seems remarkable that the process of crystal growth is between 1-5 min, but we must consider that the deposited crystallization product is a non-conductive material. The impact of the electrochemical strategy focuses on the early events of crystallization, which it is strongly influenced by the generation of crystallization nuclei, which are then developed by non-conventional electrochemical pathways. That is why the results are outstanding and showing that we can control the mineralization process with a given current. Electrocrystallization can be performed at short time and allow us to study various aspects of the biomineralization such as coating thickness, effects of the current density on the morphology and the structure of the coating, concentration, etc. It is also a good synthetic method to investigate morphogenetic and crystallographic aspects of crystals using extra films deposition with either biopolymer or synthetic molecules on ITO substrate under ambient condition.

Given the existence of three hydrates of CaOx, this is a good model to evaluate the electrochemistry-induced polymorph selection. For instance, Windhausen and Switzer deposited CaOx by cathodic reduction of an acidic bath, containing Ca^{2+} and $C_2O_4^{2-}$ ions [22]. They describe that CaOx precipitates at pH 5 and above. By applying current, a steep increase in the pH is observed close to the cathode due to hydrogen evolution and other companion reactions. This phenomenon was referred to as "*electrogeneration of base*" [23]. Thus, COM crystals were deposited on the cathode and also COT was crystallized using high degrees of supersaturation brought about by enhancing the bath concentration [24, 25]. Joseph and Kamath evaluated how the electro-deposition parameters could affect the phase selection among the CaOx hydrates [26].

It is well known that size, phase, and morphology of CaOx crystals are controlled not only by the type of used crystallization technique such as gas and double diffusion methods, kitano method, etc. in the classical crystallization theory but also by the variation of experimental parameters e.g. molar concentration of reactants, additive, temperature, time, order of adding and molar ratio of the reactants, pH, etc. [27]. In addition, time deposition of inorganic material can be change from min to days in the classical crystallization theory.

The present work was undertaken to induce electrocrystallization of CaOx modifying the current from 6 to 24 mA at room temperature in a closed cell electrocrystallization set-up. By this approach we pretend to establish an efficient method towards stabilizing COM and COD crystals deposited on the surface of indium-tin-oxide (ITO) substrate.

Experimental

A set of CaOx electrocrystallization trials were performed at room temperature modifying the voltage from 6 mA to 24 mA in closed electrocrystallization system. The electrocrystallization of CaOx were carried out by using ethylenediaminetetraacetic acid (EDTA), sodium oxalate ($Na_2C_2O_4$) from Sigma-Aldrich and calcium nitrate tetrahydrate ($Ca(NO_3)_2 \times 4\ H_2O$) from Merck. All reagents were of the highest available grade. These solutions were sonicated during 5 min in an ultrasonic cleaner Bronson 200. $Ca(NO_3)_2$ and EDTA solutions were

first mixed and the resultant pH was adjusted to 10.5 with few drops of 1 M NaOH. This solution was mixed with $Na_2C_2O_4$ solution and then 25 ml of the resulting solution was poured into the glass electrochemical cell (ECC). Before beginning the electrocrystallization, the system was purged with oxygen (O_2) flux for 30 min. The ECC measurements were conducted in small pieces of ITO glass acting as a working electrode (WE). A coiled platinum (Pt) wire was used as auxiliary electrode (AE) and a silver chloride electrode (Ag/AgCl) as reference (RE). ITO from Corning® aluminosilicate glass, 25× 25×1.1 mm, coated with one surface of RS=5-15 Ω was used. Chronopotentiometry was used during the CaOx electrocrystallization in a galvanostat / potentiostat BASi Epsilon (USA) instrument. The used potentiostatic pulse was±10 V, with a sample interval of 2 s and current convention IUPAC. SEM images of CaOx crystals were observed in a FEI model inspect F50 and in a Tesla 343 A scanning electron microscope (SEM) instruments. Powder X-ray diffraction (PXRD) was performed by using a Siemens D-5000X X-ray diffractometer with Cu-K radiation (graphite monochromator) and an ENRAF Nonius FR 590. The crystal structure of CaOx was determined by using Cu-K α radiation (40 kV), steps of 0.02°, and the geometric Bragg–Brentano (θ–θ) scanning mode with an angle (2θ) range of 6–80° with step time of 189 s at 25 °C. The DiffracPlus program was used as data-control software.

Results and discussion

Previous studies reported in the literature on the electrocrystallization of CaOx have been performed by cathodic reduction of acidic aqueous solutions containing Ca^{2+} and $C_2O_4^{2-}$ ions [22, 24, 25]. On the other hand, in situ electrocrystallization of Ca-salts particles such as calcium carbonate ($CaCO_3$) have been also developed [28]. An excellent critical review in the area of electrocrystallization-nucleation, and concepts such as half-crystal position mean and growth of metals, alloys and the history of electrocrystallization phenomena can be reviewed by Milchev [29]. Here, we used an alternative electrochemical approach of the electrosynthetic method described by Joseph and Kamath [26]. We have tested argon and oxygen (O_2) gases to purgue electrolyte solutions during the electrocrystallization experiments. The results shown for open circuit potential is consistent with a reversible modification of the interface, where low mineralization is expected from solution conditions, however, no-change in the interface potential was observed after 5 min. The saturation of solution with O_2 for 30 min was performed in order to reach the thermodynamic equilibrium and to improve the electrochemical response. In addition, effect of polyacrilic acid (PAA) on $CaCO_3$ crystallization through ITO substrates using O_2 gas has also been evaluated in our group (unpublished results). Electrocrystallization of $CaCO_3$ implies the use of an electrolytic solution with O_2, at pH alkaline and environmental temperature. The application of negative potential at the beginning of the reaction implies the O_2 reduction in the electrode surface immediacy. By this way, O_2 electro-reduction is produced, promoting a local increase in the solution pH close to the electrode (interface electrode-solution), which in turn promotes that bicarbonate ions render to carbonate ion in the interface reaching the precipitation of $CaCO_3$ by using a calcium source. In case of CaOx electrocrystallization, different [EDTA]/[Ca^{2+}] ratios were used to obtain the Ca-EDTA complex. This complex has high stability constant with pK= 10.59 at pH 7, whereby CaOx crystallization is suppressed in pH range 5-13. Therefore, EDTA constitutes a useful tool to tune the concentration of Ca^{2+} in the electrolyte solution by varying the [EDTA]/[Ca^{2+}] ratio. Therefore, the different potential (V) obtained when current from 6 to 24 mA was applied (see Fig. 2) can be explain by the concentration ratio of $Ca(NO_3)_2$: $Na_2C_2O_4$: EDTA, which controls the different [EDTA]/[Ca^{2+}] ratios, which is a critical point for the stabilization of Ca-EDTA complex. CaOx deposition starts when pH decreases. We found that the value of pH solution was a key parameter during the electrocrystallization. pH value influence the CaOx deposition, which starts on the ITO and permit the acid hydrolysis of Ca-EDTA complex releasing the Ca^{2+} ions into solution. Therefore, electrocrystallization at acid pH is generated at the WE (anode) by the breaking of water molecules, generating free O_2 and protons [30]. The Ca-EDTA complex stability decreases as the pH value decreases, releasing the Ca^{2+} ions by acid hydrolysis of Ca-EDTA complex. By this way, the free Ca^{2+} ions react with oxalate ions getting CaOx particles as locally deposited on the WE surface. Equations 1-4 clarify the electrocrystallization of CaOx on ITO surface.

$$Ca(NO_3)_2 + EDTA{-}4Na \xrightarrow{pH=10.5} Ca{-}EDTA{-}2Na + 2Na^+ + 2NO_3^- \quad (1)$$

$$Ca{-}EDTA{-}2Na + 2Na^+ + 2\ NO_3^- + Na_2C_2O_4 \xrightarrow{O_2\times 30\ min} No\ \ Reaction\ \ Occurs \quad (2)$$

$$2\ H_2O \xrightarrow{\text{A=6 mA}} O_2 + 4H^+ + 4e^- \quad (3)$$

$$Ca-EDTA{-}2Na + 2Na^+ + 2NO_3^- + Na_2C_2O_4 + 4H^+ \xrightarrow{pH\le 5.0} CaC_2O_{4(s)} + EDTA{-}4Na + 2NO_3^- + 2Na^+ + 4H^+ \quad (4)$$

ITO substrate is a popular material that is useful for many opto-electronic applications using different substances and nanoparticles materials [31–33]. We used ITO because is an

electrode widely used in electrochemistry due to its excellent optic transparence, high electric conductivity, wide work window in electrochemical studies and high physical and electrochemical stability [34, 35]. ITO has been also used as WE in electrocrystallization of $CaCO_3$ test [36] as described the method reported by Lédion et al. [37], where consists in the deposition of $CaCO_3$ on WE substrate, by using a fixed negative potential in relation to reference electrode (RE). In case of electrocrystallization of $CaCO_3$, electrodes used are composed of carbon surface or those covered by oxide, such as electrodes made from ITO. The formed inorganic deposit, which is no conductive, reduces the electrode active area, constituting a barrier for oxygen diffusion. Then, total cathodic current decreases and can be followed by chronoamperometric measurements [38]. The registered current could be analyzed according to its variations in time, in fact, it is possible to identify when the surface of electrode is covered totally by crystals, and since chronoamperometric curves are obtained. On the other hand, Dickey et al. [39] described the controlled fabrication of ordered arrays of nanotubes of ITO materials for electro-optical applications such as sensors and photovoltaics. In this sense, recently, Anoop et al. described its use in a molecular electronic device with quantum dots (QD) and fullerenes, with a promising performance, as well [40]. Electrochemical technique is an appropriate and relatively simple method leading to the formation of natural and synthetic nanostructured deposit on ITO substrate [41, 42]. We also employed ITO subtrates due to its technical reasons in electrocrystallization experiments on inorganic materials such as $CaCO_3$ and CaOx.

The applied current utilized during chrono-potentiometric studies was based on published work by S. Joseph and P. V. Kamath (2008). These authors electrodeposited CaOx hydrates by using electrogeneration of acid at the anode from an EDTA-stabilized calcium nitrate bath, containing dissolved oxalate ions [26]. They controlled selectively the polymorphism of CaOx by fixing the following conditions: pH (9 and 11), temperature (~23 and 65 °C) and current density (3 mA and 6 mA) of the electrolyte solution. The authors indicated that the stabilization of COD was favored with 6 mA/cm^2 at 23 °C, whereas the formation of COM crystals was promoted with 3 and 6 mA/cm^2 at 65 °C. Both polymorphs showed oriented growth with respect to the substrate under different deposition conditions. These authors hypothesized that COD is formed first, then it transforms to COM in a similar manner as in nature, namely by dissolution/reprecipitation mechanism. COM crystals were stabilized at pH 11 and 6 mA / cm^2 at 65 °C. It is well known that cyclic voltammetry is crucial for evaluating the current vs. potential profiles in Ca-based solution and in solution free of Ca^{2+} or even though in the electrodeposition of natural and synthetic polymers but in the current was not performed. In this context, we have recently used chitosan as template for the electrocrystallization of CaOx in our group (unpublished results). Electrocrystallization of CaOx was performed as is illustrated in Fig. 1 and the experimental conditions are summarized in Table 1.

Table 1 shows the experimental conditions used for the crystal growth of CaOx performed through electrocrystallization by varying the reagents ratio and current.

Fig. 2 shows the chronopotentiometry of CaOx samples A-C, E-J and L (Table 1). Data in Table 1 shows different potential curves when 6, 12, 18 and 24 mA were applied during 1 to 5 min. Data corresponding to samples D and K were not included in Fig. 2 due to an accidentally experimental error occurred while handling the WE during the chronopotentiometric measurement. We found that, for all reactant ratios and applied current the range of 0.9 to 2.1 mV, different type of CaOx crystals were growth and deposited on ITO substrate. In general, chronopotentiometry curve revealed an increase in the potential value for all samples during the in vitro electrocrystallization test. In addition, it is clear that for samples C and F, both with higher ratio of $Ca(NO_3)_2$:$Na_2C_2O_4$:EDTA (50:50:75), a constant chronopotentiometric curve was observed during the whole electrocrystallization essay, when 6 and 12 mA current was applied, respectively.

The chronoamperometry curves show indirect nuclei generation rate of crystallization. So for a given electrolyte composition as F, I and L, the increase in current interface shows that at low current densities can generate a progressive nucleation with a slow changing in the interface on the other side high current densities show an evolution potential in the direction of an instantaneous nucleation which generates multiple structures simultaneously. We found for these samples that starting potential (V) value was 1.74, 1.52 and 0.94 V, and the final potential data of 1.84, 2.07 and 1.72 V, respectively. The chronopotentiometry curve revealed an opposite starting potential respect to the applied current; however, for all these samples an increase in the chronopotentiograms evolution during the electrocrystallization was registered. Sample L showed that the increasing in the potential curve was more pronounced when 24 mA was applied. Its chronopotentiometry curve had a fast increasing of potential value at the initial of experiment less than 1 min (a fifth of one min) and then its potential curve reached the final value of 1.72 V. Chronopotentiometry of sample F presented a flat evolution curve of 0.55 V between the starting and final potential data when 12 mA was applied. The chronopotentiometric curve of sample I showed a similar behavior of sample L but with greater final potential data. In the case of sample A with the lowest ratio of reactants (10:10:15) and applied current, the chronopotentiometric curve had a fast increasing at the initial of experiment *ca.*1 min and then a slight decay until its potential curve reached a constant behavior at the end of the

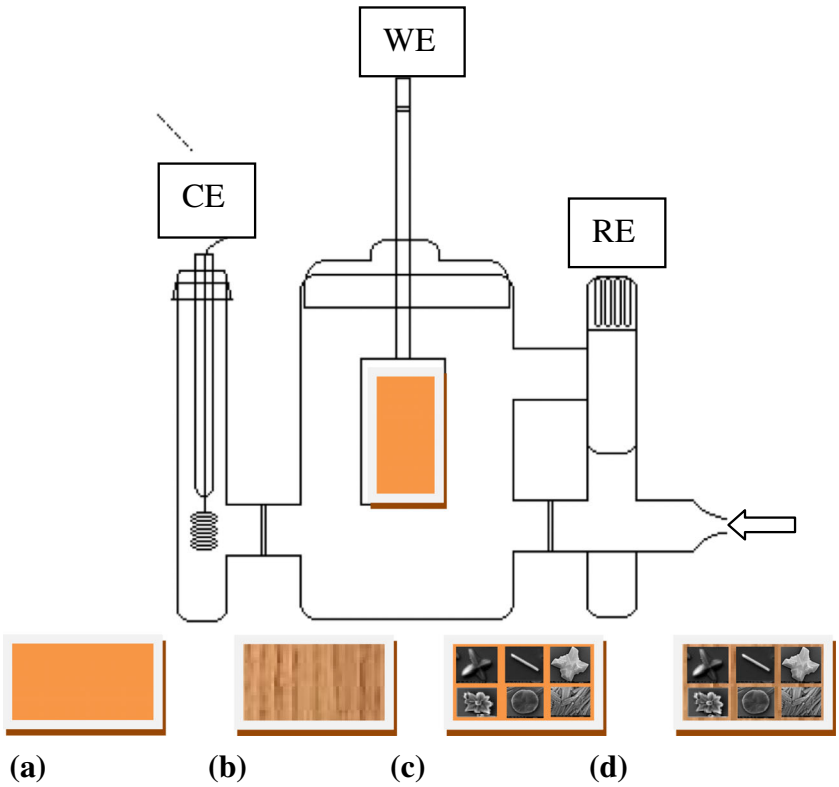

Fig. 1 Experimental set-up for the electrocrystallization of CaOx. ITO (**a**), electrodeposition of polymer on ITO (**b**), electrocrystallization of CaOx on ITO (**c**) and electrocrystallization of CaOx on electrodeposited polymer - ITO (**d**)

experiment *ca*.5 min. It may also be distinguishable that when higher ratio of reagents for samples B, E and I was used, the chronopotentiometric curve showed higher values of potential in the range of 1.7 to 2.0 V. In addition, the distribution and type of CaOx crystals on WE surface was more homogeneous, where isolated COD crystals with well-defined shapes and edges were obtained. The chronopotentiometry measurements suggests that current as low as 6 mA would be enough to gather the water hydrolysis, decrease the local pH of electrolyte solution at the interface of WE promoting the crystal growth of CaOx on ITO substrate. For increasing EDTA concentration and applied current from 6 to 24 mA, we did not find a predictable performance regarding the stabilization of COD crystals, however new shape, nano-organization and increasing growth of the non-pathological COD crystal was promoted at room temperature (23 °C). In order to provide more insights, we have performed various CaOx electrocrystallization tests by using similar reactant ratios as above, lower current than 6 mA, different temperatures and changing the cell electrocrystallization set-up to study the deposition.

Table 1 Electrocrystallization of CaOx on ITO substrate. Concentrations of reagents were carried out in mMol/L

Samples	Reagents	Ratio	Current mA
A	$Ca(NO_3)_2 : Na_2C_2O_4 : EDTA$	10 : 10 : 45	6
B	$Ca(NO_3)_2 : Na_2C_2O_4 : EDTA$	30 : 30: 45	6
C	$Ca(NO_3)_2 : Na_2C_2O_4 : EDTA$	50 : 50 : 75	6
D	$Ca(NO_3)_2 : Na_2C_2O_4 : EDTA$	30 : 30 : 45	12
E	$Ca(NO_3)_2 : Na_2C_2O_4 : EDTA$	40 : 40 : 60	12
F	$Ca(NO_3)_2 : Na_2C_2O_4 : EDTA$	50 : 50 : 75	12
G	$Ca(NO_3)_2 : Na_2C_2O_4 : EDTA$	30 : 30 : 45	18
H	$Ca(NO_3)_2 : Na_2C_2O_4 : EDTA$	40 : 40 : 60	18
I	$Ca(NO_3)_2 : Na_2C_2O_4 : EDTA$	50 : 50 : 75	18
J	$Ca(NO_3)_2 : Na_2C_2O_4 : EDTA$	30 : 30 : 45	24
K	$Ca(NO_3)_2 : Na_2C_2O_4 : EDTA$	40 : 40 : 60	24
L	$Ca(NO_3)_2 : Na_2C_2O_4 : EDTA$	50 : 50 : 75	24

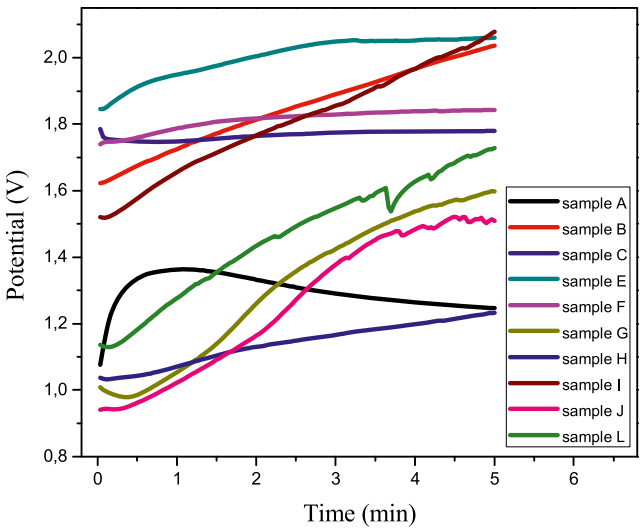

Fig. 2 Chronopotentiometry of CaOx

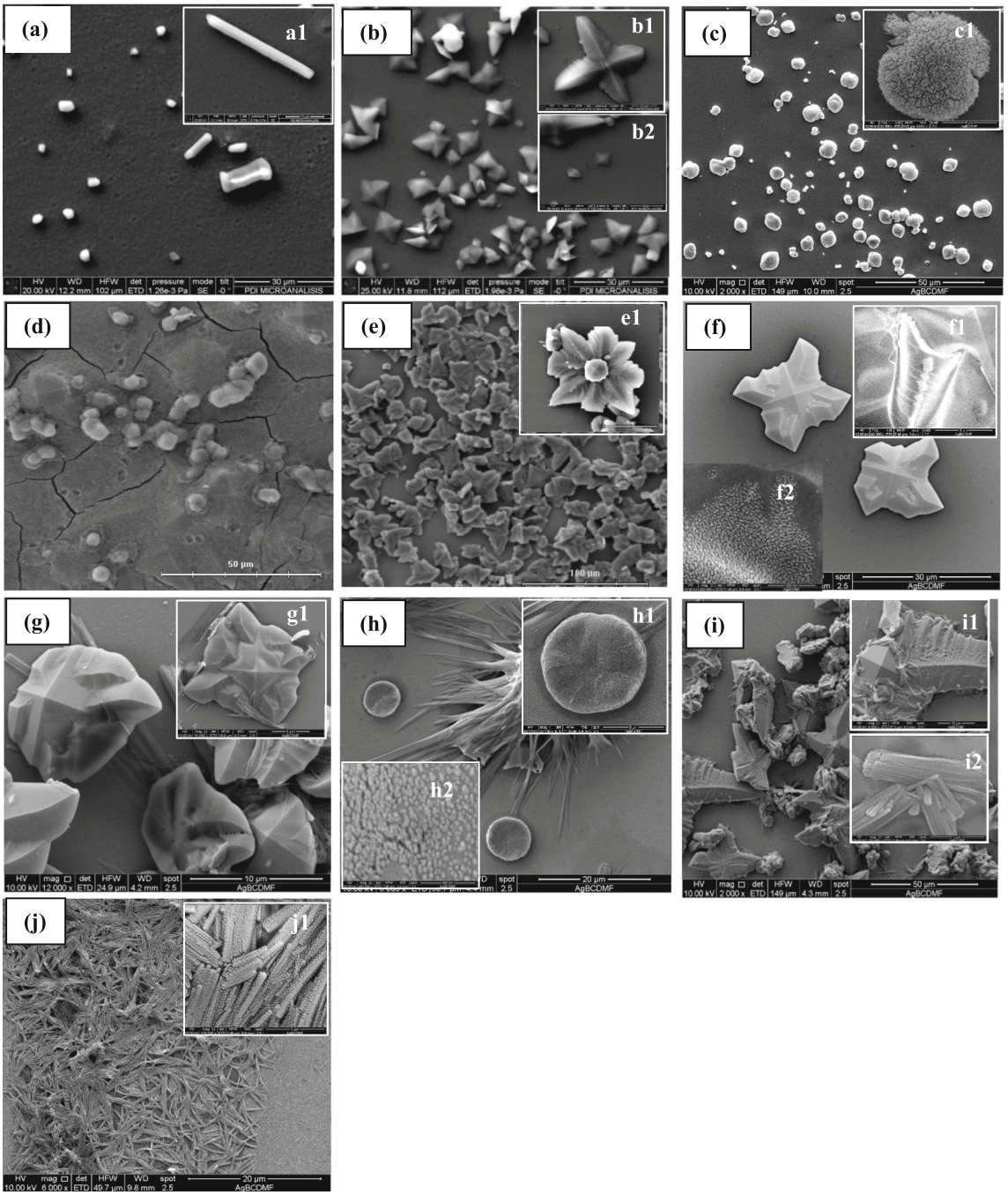

Fig. 3 SEM images of CaOx crystals obtained by electro-crystallization. Morphology and shape of these crystals are representative of the entire sample population, while their size can be diverse from the average. Sample A (**a**), sample B (**b**), sample C (**c**); sample E (**d**), sample G (**e**), sample H (**f**), sample I (**g**), sample J (**h**), sample K (**i**), and sample L (**j**)

The morphology (Fig. 3) and polymorphism (Fig. 4) of CaOx crystals were evaluated through scanning electron microscopy (SEM) and powder X-ray diffraction (XRD) techniques, respectively. Fig. 3 shows the SEM images of CaOx crystals obtained by electrocrystallization of representative samples obtained by applying 6, 12, 18 and 24 mA. In general, the experimental condition and the type of sample used show considerable effects on the morphology of the resultant CaOx crystals in the absence of additives. Fig. 3a shows the formation of small (~2-5 μm) and micro rod-like COD crystals (~20 μm) on ITO when sample A (10:10:30) and 6 mA current was applied. These elongated COD crystals have been previously reported in the presence of a synthetic block copolymer [15]. The elongation take place due to the stabilization of {100} faces from tetragonal bipyramid crystals dominated by the {101} face [15]. They found that rod-like COD crystals

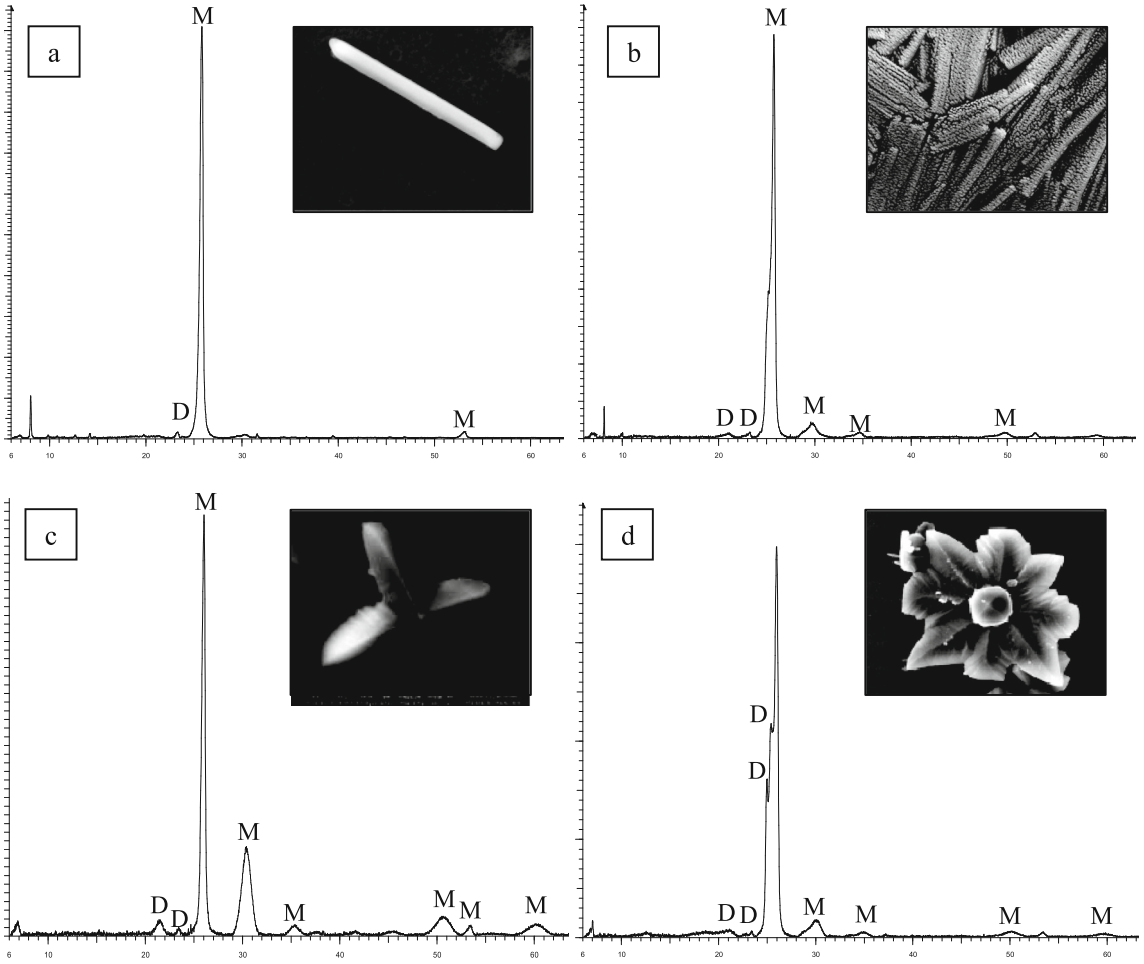

Fig. 4 XRD patterns of the CaOx crystals grown on ITO substrate. Sample A (**a**), sample L (**b**), sample B (**c**), sample G (**d**). Peaks characteristic of COM and COD were labeled as "M" and "D", respectively

are kinetically favored in solutions. In Fig. 3b we observe homogenous distribution of typical micro COD crystals (~10 μm) with well-developed tetragonal prisms on ITO in the presence of sample B (30:30:40) when 6 mA was applied. Surprisingly, as seen in Fig. 3c, regular and homogenously distributed dumbbell-shaped CaOx crystals (~5 μm) were formed on ITO in the presence of sample C and 6 mA current. It should be noted that this sample is composed of much higher electrolyte reagent ratio (50:50:75). These CaOx crystals showed nano-regular pointed tips structure, which apparently are formed by the assembly of nano and micrometer units on the CaOx surface. These leads to the spherical dumbbell-like CaOx particles. In Fig. 3d, few and irregular CaOx crystals in the range of ~10 μm in size are observed on ITO in the presence of sample E (40:40:60) when 12 mA was applied. On the other hand, distinct morphological COD with slight crystalline shape for samples G, H and I occurred when 18 mA current was applied. Unexpectedly, unusual and regular COD flower- like crystals in the range of 10 to 20 μm in size were formed when sample G (30:30:45) was used (Fig. 3e). This crystals shape appearance enabled to distinguish the tetragonal bipyramid having central part as square base, typical of COD crystals. We note that the number of petals of the flower-shaped crystal can vary from 2 to 8. On the other hand, in the presence of sample H (40:40:60), characteristic CaOx crystals with "swirl" peripheral growth and more defined vertices were deposited on the WE surface (Fig. 3f). These crystals correspond also to COD with the tetragonal bipyramid as a central nucleation point, which has slightly lost the flower-crystal appearance. At high magnification (see f1and f2), selected "*swirl*" crystal is observed, which exhibit multiple foci arranged in ventral crystalline faces, corresponding to nanometer clusters arrangement (18-24 nm). In the presence of sample I, (50:50:75) similar COD crystals with size of 5 to 10 μm were observed when 18 mA current was applied (Fig. 3g). At the end, Fig. 3h, i and j shows that when the highest current 24 mA was applied COD, circular and CaOx-parallelepiped like crystals for samples J, K and L were

crystallized on ITO, respectively. Unpredictably, the Fig. 3h, shows the formation irregular filamentous and circular CaOx crystals (~5 to 7 μm) on ITO substrate, which were formed in the presence of sample J (30:30:45) when 24 mA current was applied. These CaOx crystals showed nano-regular structure (18-25 nm), which appears as a self-assembly of nano and micrometer CaOx units crystallized on the ITO surface (Fig. 3h1 and h2). Fig. 3i shows SEM images of irregular COD crystals grown in the presence of sample K (40:40:60) when 24 mA current was applied. Here we observed different sub-micron and micro parallelepiped (Fig. 3i1 and i2) crystals deposited on the COD-petals. We also observed "*swirl*" morphology with extended petals-shaped morphology for CaOx at this current. Finally, abundant sub-micron and micro parallelepiped (3j1) crystals were formed in the presence of the highest concentration ratio (50:50:75) of reagents and applied 24 mA current (Fig. 3j). These parallelepiped-shape CaOx crystals are in turn composed of countless unique and independent nanocrystals.

As we known XRD is a more suitable technique than electron microscopy to identify inorganic constituents in kidney stones by their unique diffraction patterns, which allows definite identification of crystalline substances unknown. Therefore, XRD was used in our electrocrystallization study to confirm the most representative electron microscopic morphologies. In the Fig. 4 we selected and showed the XRD patterns of samples A, B, G and L. In order to illustrate the characteristic morphologies of CaOx grown on the ITO substrate, we added the insert SEM pictures showed in the Fig.3, that is, a1, b1, e1 and j1. In general, Fig. 4 shows the XRD patterns with reflection peaks observed at around 2θ=8°, 21.5°, 22.8°, 24.2°, 25.8°, 30°, 35° 50°, 53° and 60° confirming the presence of COM and COD crystals [43–46]. In the Fig. 4a and b for samples A and L, it can be seen peaks at 2θ=8°, 21.5°, 22.8°, 25.8°, 30°, 50 and 53°, which are ascribed to the diffraction of mix of COM and COD crystals. We found here an unidentified reflection peak at 2θ=8°. For samples B and G with flower-like crystals morphologies, Fig. 4c and d, we found a major reflection peaks of COD at 2θ=21.5°, 23.5°, 25.8°, 30°, 35°, 50°, 53° and 60°.

Conclusions

Electrocrystallization of CaOx with different morphology and size on ITO surface at short time through chronopotentiometry was obtained. The control of the experimental parameters such as electrical current, concentration of reactants, time and electrochemical cell type allowed us to induce selective crystallization of COM and COD. The morphology of COD crystals was strongly influenced by the concentration ratio of $Ca(NO_3)_2$:$Na_2C_2O_4$:EDTA and the applied current from 6 to 24 mA at 23 °C. In summary, we demonstrated that without the use any additives during the electrocrystallization process, CaOx crystals with self-assembly organization at nano/micro scale were obtained.

Acknowledgements This research was supported by FONDECYT 1140660, FONDAP ACCDiS 15130011 granted by the Chilean Council for Science and technology (CONICYT) and funded by Program U-Redes, Vice-presidency of Research and Development, University of Chile. Authors M. Sánchez and P. Vásquez-Quitral also thank to CONICYT Scholarship.

References

1. DiMasi E, Gower LB (2014) Biomineralization sourcebook - characterization of biominerals and biomimetic materials, 1st edn. CRC Pres, Taylor & Francis Group, Florida
2. Lieske J, Leonard R, Toback G (1995) Renal fluid electrolyte. Am J Physiol 37:604
3. Karlsen SJ, Grenabo L, Holmberg G, Colstrup H, Jorgensen TM, Lindell O, Ala-Opas M, Ulvik NM, Shultz A, Griffith DP (1995) J Urol 153:378
4. Wesson JA, Ward MD (2007) Elements 3:415
5. Neira-Carrillo A, Vásquez-Quitral P (2010) Av Cs Vet 25:41
6. Long LO, Park S (2007) Minerva Urol Nefrol 59:317
7. Monje P, Baran E (2002) Plant Physiol 128:707
8. Tomažic B, Nancollas GH (1979) J Cryst Growth 46:355
9. Wesson JA, Worcester EM, Wiessner JH, Mandel NS, Kleinman JG (1998) Kidney Int 53:952
10. Finlayson B (1978) Kidney Int 13:344
11. Benitez IO, Talham DR (2004) Langmuir 20:8287
12. Benitez IO, Talham DR (2005) J Am Chem Soc 127:2814
13. Khan SR, Whalen PO, Glenton PA (1993) J Cryst Growth 134:211
14. Brown CM, Novin F, Purich DL (1994) J Cryst Growth 135:523
15. Zhang D, Qi L, Ma J, Cheng H (2002) Chem Mater 2450:2450
16. Golden TD, Shumsky MG, Zhou Y, VanderWerf RA, Leeuwen RAV, Swizter JA (1996) Chem Mater 8:2499
17. Joseph S, Kamath PV (2008) Solid State Sci 10:1215
18. Rudnik E (2013) Ionics 19:1047
19. Saha S, Sultana S, Islam MM, Rahman MM, Mollah MYA, Susan MABH (2014) Ionics 20:1175
20. Gebauer D, Völkel A, Cölfen H (2008) Science 322:1819
21. Gebauer D, Kellermeier M, Gale JD, Bergstro L, Cölfen H (2014) Chem Soc Rev 43:2348
22. Windhausen AB, Swizter JA (2008) Abstracts, 64th southwest regional meeting of the american chemical society. Little Rock, AR, United States
23. Swizter JA (1987) Am Ceram Soc Bull 66:1521
24. Kajita T, Kogyo N-S (1995) Kenkyusho Kenkyu Hokoku 80:22
25. Kajita T (1989) Hyomen Kagaku 10:181
26. Joseph J, Kamath PV (2009) J Solid State Electr 14:1481
27. Thongboonkerd T, Semangoen T, Chutipongtanate S (2006) Clin Chim Acta 367:120
28. Euvrard M, Filiatre C, Crausaz E (2000) J Cryst Growth 216:466
29. Milchev A (2011) J Solid State Electr 15:1401
30. Dinamani M, Kamath PV, Seshadri R (2003) Solid State Sci 5:805
31. Jo K, Yu HZ, Yang H (2011) Electrochim Acta 56:4828
32. Yang G, Yang Y, Wang Y, Wang Y, Yu L, Zhou D, Jia J (2012) Electrochim Acta 78:200
33. Anipa TN, Anoop KM, Pai RK (2015) New J. Chem. DOI: 10.1039/C5NJ01350J
34. Zhang J, Oyama M (2005) Anal Chim Acta 540:299

35. Ma Y, Di J, Yan X, Zhao M, Lu Z, Tu Y (2009) Biosensors and Bioelectronics 24:1480
36. Pavez J, Silva J, Melo F (2005) Electrochim Acta 50:3488
37. Lédion J, Leroy P, Labbe JP (1985) TSM L´eau 80:323
38. Ketrane R, Saidani B, Gil O, Leleyter L, Baraud F (2009) Desalination 249:1397
39. Dickey MD, Weiss EA, Smythe EJ, Chiechi RC, Capasso F, Whitesides GM (2008) ACS Nano 2:800
40. Anoop KM, Mohanta K, Pai RK (2014) IEEE J Photovolt 4:1570
41. Aoki Y, Huang J, Kunitake T (2006) J Mater Chem 16:292
42. Cheng Z-X, Dong X-B, Pan Q-Y, Zhang J-C, Dong W (2006) Mater Lett 60:3137
43. Zhang D, Qi L, Ma J, Cheng H (2002) Chem Mater 14:2450
44. Kirboğa S, Öner M (2009) Cryst Growth & Design 9:2159
45. Kumar N, Singh P, Kumar S (2006) Indian J Biochem Bio 43:226
46. Neira-Carrillo A, Vásquez-Quitral P, Fernández MS, Luengo-Ponce F, Yazdani-Pedram M, Cölfen H, Arias JL (2015) Eur. J. Inorg. Chem. 2015/7:1167